Bell, David R.; Ledoit, Olivier; Wolf, Michael

Working Paper

A novel estimator of earth's curvature (allowing for inference as well)

Working Paper, No. 431

Provided in Cooperation with:
Department of Economics, University of Zurich

Suggested Citation: Bell, David R.; Ledoit, Olivier; Wolf, Michael (2023) : A novel estimator of earth's curvature (allowing for inference as well), Working Paper, No. 431, University of Zurich, Department of Economics, Zurich,
https://doi.org/10.5167/uzh-232795

This Version is available at:
https://hdl.handle.net/10419/275649

University of Zurich[UZH]

University of Zurich

Department of Economics

Working Paper Series

ISSN 1664-7041 (print)
ISSN 1664-705X (online)

Working Paper No. 431

A Novel Estimator of Earth's Curvature (Allowing For Inference As Well)

David R. Bell, Olivier Ledoit and Michael Wolf

April 2023

A Novel Estimator of Earth's Curvature (Allowing For Inference As Well)

David R. Bell
Idea Farm Ventures
18 W. 18th Street
New York, NY 10011, USA
david@ideafarmventures.com

Olivier Ledoit
Department of Economics
University of Zurich
8032 Zurich, Switzerland
olivier.ledoit@econ.uzh.ch

Michael Wolf
Department of Economics
University of Zurich
8032 Zurich, Switzerland
michael.wolf@econ.uzh.ch

April 1, 2023

Abstract

This paper estimates the curvature of the Earth, defined as one over its radius, without using *any* physics. The orthodox model is that the Earth is nearly spherical with a curvature of $\pi/20,000$ km. By contrast, the heterodox flat-Earth model stipulates a curvature of zero. Abstracting from the well-worn arguments for and against both models, rebuttals and counter-rebuttals *ad infinitum*, we propose a novel statistical methodology based on verifiable flight times along regularly scheduled commercial airline routes; this methodology allows for both estimating and making inference for the curvature. In particular, a formal hypothesis test resolutely rejects the flat-Earth model, whereas it does not reject the orthodox spherical-Earth model.

KEY WORDS: Flat-Earth model, geodesy, nonlinear least squares, trigonometry.

JEL classification codes: C12, C13.

1 Introduction

This paper develops a novel and first-of-its-kind statistical methodology to learn about Earth's curvature (and thus about its radius as well, one being the reciprocal of the other); estimation is the first step, followed by formal inference as a second step. In particular, this methodology allows us to carry out a powerful, easily verifiable, and even-handed test of the flat-Earth model vs. the spherical-Earth model. There are at least three strong reasons to write, read, or publish this paper — each either overturns a weak objection or negates reliance on an appeal to authority.

First: The flat-Earth model is heterodox whereas the spherical-Earth model is orthodox. This objection is weak because, by the nature of scientific revolutions, all theories currently accepted as orthodox started with the minority opinion of one single person (or group) who disagreed with then-prevailing orthodoxy. Such process will continue as long as civilization perdures. What this implies, however, is that very few of the many heterodox opinions bubbling up will survive tough tests. On this basis, the challenge is to design a test that is most powerfully conclusive, and this is what we do in the present paper.

Second: The flat-Earth model is a conspiracy theory. This objection is weak because many conspiracies that were once alleged to be theories later turned out to be validated by facts. For example, the Donation of Constantine was used during the Middle Ages by the Roman Catholic Church to justify its temporal control over Italy. It was only exposed as a fraudulent conspiracy centuries later during the Renaissance by Lorenzo Valla. Many conspiracy theories will turn out to be false, but only by extending to all of them an even-handed treatment can we fish out the few that may later turn out factual.

Third: The flat-Earth model is easily rejected by the testimony of astronauts, Antarctica explorers, Navy captains, and other high-level specialists whose careers depend on espousing the correct model of the shape of the Earth. This is a powerful objection, but one not accessible to the educated layman whose everyday knowledge lies elsewhere. Therefore, a statistical test that relies only on high-school trigonometry and easily downloadable commercial flight data is much more convincingly general in its reach.

To the best of our knowledge, a test of the flat-Earth hypothesis against the spherical-Earth hypothesis has not yet been conducted in the most solid and convincing way which requires: (i) a simple yet powerful design; (ii) easily verifiable and uncontroversial data; and (iii) execution in an even-handed and disinterested way. The present paper fills this gap. Naturally, theoretical physicists have weighed in on the debate; for example, see Kuzii and Rovenchak (2019). The beauty of our approach is that we can resolve the argument without any recourse to physics whatsoever; in particular, our purely statistical

methodology also produces an estimator of Earth's radius (which is the reciprocal of Earth's curvature) that enjoys near-perfect accuracy.

The paper unfolds as follows. Section 2 develops a general formula for the distance between two points on Earth that embeds both the flat model and the spherical model as special cases of a 'curvature' parameter. Section 3 accurately calibrates a specific linear mapping from kilometric distance to flight duration that should be acceptable to both flat-Earth and spherical-Earth proponents, by focusing on airline routes where they are most in agreement: the ones oriented along a North-South axis, allowing for North Pole flyover. Section 4 uses this calibration to execute a formal hypothesis test by focusing on airline routes where flat-Earth and spherical-Earth models are most in *dis*agreement: the ones oriented along an East-West axis, far from the North Pole. Section 5 concludes and reaffirms the core insight of our paper, namely that whereas travel along the North-South axis allows for model calibration and agreement between the flat-Earth and spherical-Earth models, travel along the East-West axis produces a powerful test to discriminate unambiguously between the two models. The Appendix contains all mathematical proofs, as well as supporting materials.

2 Integrated Model of Distance between Two Points

The Flat Earth Society promotes Figure 2.1 as a map of the surface of the Earth.[1]

[1] Appendix B contains other historically-famous representations of the same view from various sources.

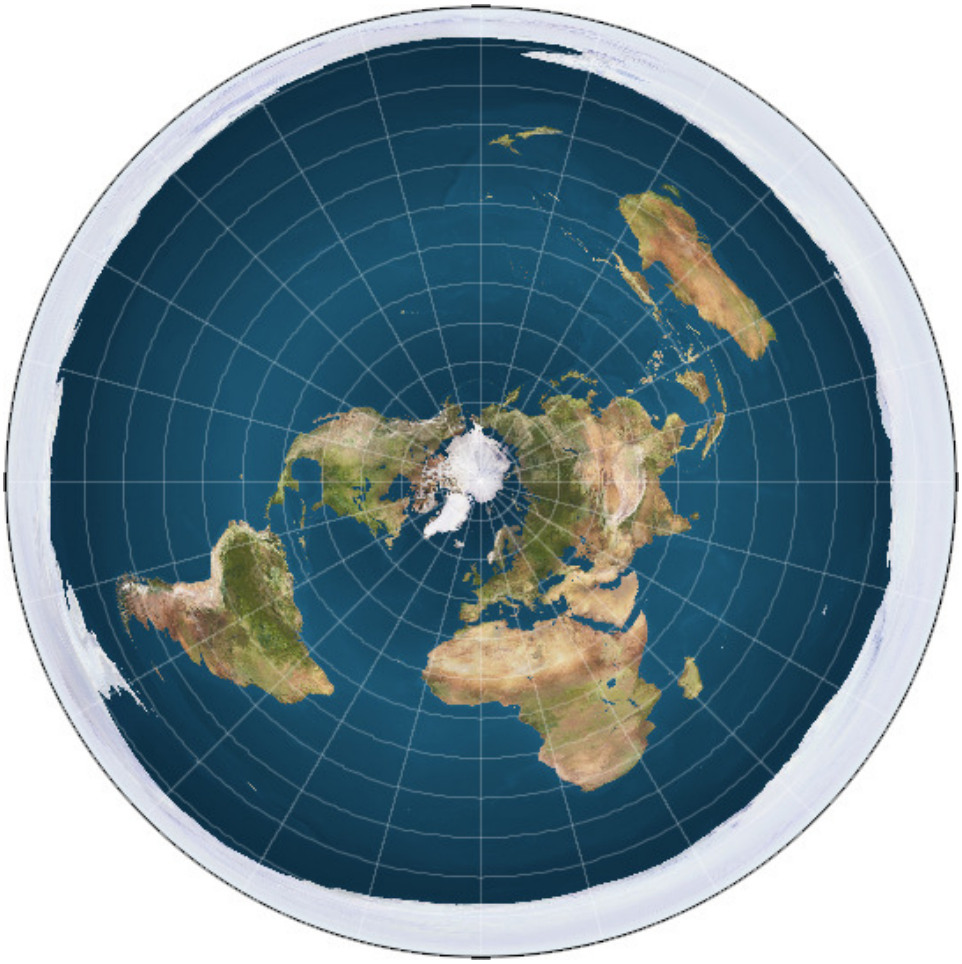

Figure 2.1: Map of the continents and oceans if the Earth is flat.

Although far from immediately obvious, especially considering the persistence of the debate and strident beliefs on both sides, analytical thinking reveals that there is a surprising amount of commonality between the flat-Earth and spherical-Earth models. Such points of agreement shall form the foundation on which a powerful test of the flat-Earth model can later be erected.

2.1 Four Cardinal Points and Longitude

The first point of agreement between the spherical-Earth and flat-Earth models is that they both agree that there is the concept of "the North". This is presumably due to the fact that a simple magnetic compass, which was available in Medieval Europe at least a century before Copernicus and Galileo, always indicates the same direction — which happens to be the same as the position of the North Star, an easily-identifiable star visible

everywhere in the Northern Hemisphere on cloudless nights.[2] If we face North, the concept of West is defined as the perpendicular direction through the left shoulder, East through the right, and South as the diametrical opposite of North.

Hereby, we deduce that the North Pole exists according in the flat-Earth model as well: If all the people on Earth walked North, this is where they would meet. Indeed, Figure 2.1 clearly shows that the North Pole is the *center* of the disk-shaped flat Earth.

An equally important point of agreement is the concept of *longitude*. It is customary to pick one specific line (properly called *meridian*) that extends away from the North Pole (going South) as reference: the *prime* meridian that goes through Greenwich near London defines 0° of longitude.[3] From the configuration of the continents, the Greenwich meridian can be clearly seen in Figure 2.1 as extending vertically downwards from the North Pole. Then, any meridian is indexed by a longitude East or West in the range $[0°, 180°]$. Not all meridians can be shown on a map, of course; the map in Figure 2.1 shows the ones that are integer multiples of 15°.

2.2 Parallel Circles

Given the symmetry of rotation, it is possible to draw circles on the surface of the Earth that contain all the points that are a given distance from the North Pole. Both spherical-Earth and flat-Earth models agree on this, although they might name them differently: "parallel circles" in the former case and "concentric circles" in the latter.

A real and substantive terminological difficulty does however emerge from the distinct labeling of the circles. In the spherical-Earth model, they are labeled by the latitude in degrees away from the equator (North or South). In the flat-Earth model, the equator exists, and can be see in Figure 2.1 as the circle running through Ecuador, the Congo, and Singapore, but it has no special pride of place relative to the other circles.

The reconciliation comes from realizing that Figure 2.1 is a polar azimuthal equidistant projection (Snyder, 1987, p. 192). This means that all points on the map are at the distance from the North Pole stipulated by the spherical-Earth model. If we list the eleven circles visible in Figure 2.1 by order of increasing radius, we get the following table of correspondence between the flat-Earth and spherical-Earth nomenclatures.

[2] There is a difference between the geographic North and the magnetic North, but it is so small that we need not take it into account here.

[3] In 1984, the prime meridian was moved 102 meters East of its original location in the middle of the Greenwich observatory, but this does not impinge upon our analysis.

Circle Number	Latitude	Notable City	Distance from North Pole
Circle 1	75° North	Kullorsuaq (Greenland)	1,667 km
Circle 2	60° North	Kronstadt (Russia)	3,333 km
Circle 3	45° North	Minneapolis (USA)	5,000 km
Circle 4	30° North	New Orleans (USA)	6,667 km
Circle 5	15° North	Khartoum (Sudan)	8,333 km
Circle 6	0° Equator	Quito (Ecuador)	10,000 km
Circle 7	15° South	Brasília (Brazil)	11,667 km
Circle 8	30° South	Porto Alegre (Brazil)	13,333 km
Circle 9	45° South	Dunedin (New Zealand)	15,000 km
Circle 10	60° South	Base Orcadas (Argentina)	16,667 km
Circle 11	75° South	Concordia (Artanctica)	18,333 km

Table 2.1: Distance from the North Pole for eleven circles.

The fourth column computes the kth circle's distance from the North Pole as

$$\Delta_k := \frac{15k}{90} \times 10,000 \qquad \text{for } k = 1, \ldots, 11 \ . \tag{2.1}$$

This is because the meter was defined by the French Revolution as the $(1/10,000,000)^{\text{th}}$ part of the distance between the North Pole and the equator (Circle 6 in the table). An expedition was sent out to measure France from North to South along the Paris meridian, which resulted in the production of a platinum bar of one meter of length subsequently held at the Paris observatory, and available for international reference.[4] The meter thus defined is physically the same in both the flat-Earth model and the spherical-Earth model.[5]

By building on the commonalities identified between the two models, we are now ready to develop an integrated formula for the distance between any two locations on Earth.

2.3 Conversion to Polar Coordinates

The first priority is to transform latitudes and longitudes commonly expressed as degrees/minutes/seconds into polar coordinates: distance from the North Pole and longitude expressed in radians relative to the Greenwich meridian.

[4]Further expeditions and progress in geodesical technology brought international specialists to the realization that the original platinum specimen at the Paris observatory was too short. However, the difference is so small that it need not concern us here.

[5]Appendix C provides low-tech confirmation using a humble road map of the type motorists rely on to plan their trips and a hand-held measuring tape.

Proposition 2.1. *Define the constant* $c^* = \frac{\pi}{20{,}000 \text{ km}}$.

1. *If a point has latitude* $d°m's''$ *North, then its distance from the North Pole is*

$$r = \frac{\pi}{180°}\left[90° - \left(d + \frac{m}{60} + \frac{s}{60^2}\right)\right] \times \frac{1}{c^*} \ . \tag{2.2}$$

2. *If a point has latitude* $d°m's''$ *South, then its distance from the North Pole is*

$$r = \frac{\pi}{180°}\left[90° + \left(d + \frac{m}{60} + \frac{s}{60^2}\right)\right] \times \frac{1}{c^*} \ . \tag{2.3}$$

3. *If a point has longitude* $d°m's''$ *East, then its longitude expressed in radians is*

$$\theta = \frac{\pi}{180°}\left(d + \frac{m}{60} + \frac{s}{60^2}\right) \ . \tag{2.4}$$

4. *If a point has longitude* $d°m's''$ *West, then its longitude expressed in radians is*

$$\theta = -\frac{\pi}{180°}\left(d + \frac{m}{60} + \frac{s}{60^2}\right) \ . \tag{2.5}$$

These four statements are valid in both the flat-Earth model and the spherical-Earth model.

The constant $c^* := \pi/20,000$ km is equal to one over the radius of the Earth if the Earth is spherical, so it represents the *curvature* of the Earth (or, one could also say, of the meridians). If the Earth is flat, c^* does not serve to measure curvature anymore, but still serves to convert latitude into distance from the North Pole.

The main reason why we insist on defining the location of a specific point on the Earth by using the pair (r, θ) is that both the flat-Earth model and the spherical-Earth model agree on (r, θ). A supplementary reason is that (r, θ) constitute what is known as a pair of *polar coordinates*, which facilitates usage of standard trigonometric techniques.

2.4 Distance between Two Points in the Flat-Earth Model

We can now give the formula for the distance between any two points on the flat Earth.

Theorem 2.1. *Consider two points* P_1 *and* P_2 *whose respective polar coordinates are* (r_1, θ_1) *and* (r_2, θ_2). *In the flat-Earth model, the distance between these two points is equal to*

$$d^F(r_1, \theta_1; r_2, \theta_2) = \sqrt{r_1^2 + r_2^2 - 2r_1 r_2 \cos(\theta_1 - \theta_2)} \ . \tag{2.6}$$

This is what one would find by using a hand-held ruler to measure the length a straight line between any two cities on the flat-Earth map in Figure 2.1.

2.5 Distance between Two Points in the Spherical-Earth Model

To continue the parallel examination of the spherical-Earth model alongside its unorthodox flat-Earth rival, we now present a counterpart to Theorem 2.1.

Theorem 2.2. *Consider two points with polar coordinates* (r_1, θ_1) *and* (r_2, θ_2)*. In the spherical-Earth model, the distance* $d^S(r_1, \theta_1; r_2, \theta_2)$ *between these two points is equal to*

$$\frac{1}{c^*} \arccos\left\{\cos^2\left(\frac{\theta_1 - \theta_2}{2}\right)\cos\big[(r_1 - r_2)c^*\big] + \sin^2\left(\frac{\theta_1 - \theta_2}{2}\right)\cos\big[(r_1 + r_2)c^*\big]\right\}, \quad (2.7)$$

where $c^* := \frac{\pi}{20{,}000 \text{ km}}$ *is Earth's curvature in the spherical-Earth model (cf. Proposition 2.1).*

This formula is particularly intuitive in two cases:

1. When both points are on the same meridian, $\cos^2\left(\frac{\theta_1-\theta_2}{2}\right) = 1$ and $\sin^2\left(\frac{\theta_1-\theta_2}{2}\right) = 0$, so the output is the difference between the two distances from the North Pole. This corresponds to a path that does not go through either pole.

2. When the two points are on antimeridians relative to each other, $\cos^2\left(\frac{\theta_1-\theta_2}{2}\right) = 0$ and $\sin^2\left(\frac{\theta_1-\theta_2}{2}\right) = 1$, so the output depends on the sum of the two distances from the North Pole. This corresponds to a path that goes through a pole.

In the general case, since $\cos^2\left(\frac{\theta_1-\theta_2}{2}\right) + \sin^2\left(\frac{\theta_1-\theta_2}{2}\right) = 1$, the distance will be a weighted average of the distance implied by the difference $r_1 - r_2$ (not going through/near a pole), and the one implied by the sum $r_1 + r_2$ (going through/near a pole), with their relative importances controlled by the difference of longitudes $\theta_1 - \theta_2$.

2.6 Making Curvature a Free Input

This section contains our final mathematical result: an integrated formula for distance that embeds both the spherical-Earth model and the flat-Earth model as special cases, depending on how the curvature parameter is dialed up or down.

Theorem 2.3. *Define the distance function* $D\big(r_1, \theta_1; r_2, \theta_2; c\big)$ *as*

$$\begin{cases} \frac{1}{c}\arccos\left\{\cos^2\left(\frac{\theta_1-\theta_2}{2}\right)\cos\big[(r_1 - r_2)c\big] + \sin^2\left(\frac{\theta_1-\theta_2}{2}\right)\cos\big[(r_1 + r_2)c\big]\right\} & \text{if } c > 0 \\ \sqrt{r_1^2 + r_2^2 - 2r_1 r_2 \cos(\theta_1 - \theta_2)} & \text{if } c = 0 \end{cases} \quad (2.8)$$

on the domain $\{(r_1, \theta_1; r_2, \theta_2; c) \in \mathbb{R}^4 : r_1 \geq 0, r_2 \geq 0, c \geq 0, r_1 c \leq \pi, r_2 c \leq \pi\}$*. The function* D *is continuous on its domain of definition.*

The function D embeds both the spherical-Earth distance function as the special case $c = c^*$ and the flat-Earth distance function as the special case $c = 0$. Having c as a free input (parameter) will allow us to construct an estimator of Earth's curvature as well as a test of the flat-Earth model against the spherical-Earth model. In order to implement such statistical methodology in practice, we first need to identify an accurate proxy for distance that is easy to collect and verify.

3 Flight Time as Proxy for Distance between Cities

In order to validate (average) flight times of regularly-scheduled commercial aircraft as an accurate proxy for the distance between two points on the surface of the Earth in a way that is acceptable to proponents of both models, our initial focus will be on airline routes where the flat-Earth model and the spherical-Earth model most agree.

3.1 Geometric Analysis of Agreement

Pairs of locations for which both models give the same distance are identified by the following theorem.

Theorem 3.1. *Let P_1 be a point on the surface of the Earth with distance r_1 from the North Pole and longitude θ_1 expressed in decimal degrees. Similarly: $P_2 = (r_2, \theta_2)$. Then $d^F(r_1, \theta_1; r_2, \theta_2) = d^S(r_1, \theta_1; r_2, \theta_2)$ if either one of the two following conditions is satisfied:*

Condition 1: *The points are on the same meridian ($\theta_1 = \theta_2$);*
Condition 2: *The points are on antimeridians ($|\theta_1 - \theta_2| = \pi$) and $r_1 + r_2 \leq$ 20,000 km.*

3.2 Airport Pairs on North-South Axis

Manual exploration of the website flightsfrom.com yields ten commercial airline routes (listed in Table 3.1) that approximately satisfy the conditions of Theorem 3.1. The first eight satisfy Condition 1 (same meridian), and the last two satisfy Condition 2 (antimeridian, flying through the North Pole route). Distances between airports have been obtained from the original latitude and longitude data by following the derivations of Section 2. Just to illustrate, and for the sake of clarity, we can provide a fully worked-out example of the intermediary calculations for the first row of Table 3.1 between Johannesburg and Istanbul.

$$\text{Johannesburg:} \quad r_1 = 12,904 \text{ km} \qquad \theta_1 = 0.493 \text{ rad} \; ; \tag{3.1}$$

$$\text{Istanbul:} \quad r_2 = 5,415 \text{ km} \qquad \theta_2 = 0.501 \text{ rad} \; . \tag{3.2}$$

Readers are strongly encouraged to double-check these computations independently, as they are technically central to the paper.

City	Airport	Latitude	Longitude	d^{F}	d^{S}
Johannesburg (S. Africa)	JNB	26°08′00″S	28°15′00″E	7,489 km	7,489 km
Istanbul (Turkey)	IST	41°15′44″N	28°43′40″E		
Santiago (Chile)	SCL	33°23′34″S	70°47′08″W	8,238 km	8,232 km
New York (USA)	JFK	40°38′23″N	73°46′44″W		
Frankfurt (Germany)	FRA	50°02′00″N	08°34′14″E	4,561 km	4,560 km
Abuja (Nigeria)	ABV	09°00′24″N	07°15′47″E		
Abu Dhabi (UAE)	AUH	24°25′59″N	54°39′04″E	3,237 km	3,236 km
Mahé (Seychelles)	SEZ	04°40′28″S	55°31′19″E		
London (UK)	LHR	51°28′39″N	00°27′41″W	5,097 km	5,097 km
Accra (Ghana)	ACC	05°36′17″N	00°10′03″W		
Melbourne (Australia)	MEL	37°40′24″S	144°50′36″E	8,191 km	8,173 km
Tokyo (Japan)	NRT	35°45′55″N	140°23′08″E		
Hong Kong (China)	HKG	22°18′32″N	113°54′52″E	6,039 km	6,032 km
Perth (Australia)	PER	31°56′25″S	115°58′01″E		
Cape Town (S. Africa)	CPT	33°58′10″S	18°35′50″E	9,433 km	9,386 km
Frankfurt (Germany)	FRA	50°02′00″N	08°34′14″E		
Dubai (UAE)	DXB	25°15′10″N	55°21′52″E	13,403 km	13,390 km
Los Angeles (USA)	LAX	33°56′33″N	118°24′29″W		
Doha (Qatar)	DOH	25°16′23″N	51°29′36″E	12,994 km	12,983 km
San Francisco (USA)	SFO	37°37′08″N	122°22′30″W		

Table 3.1: Ten airport pairs with essentially identical flat-Earth and spherical-Earth distances.

Disagreement between the flat-Earth model and the spherical-Earth model is exceedingly small for all of the ten flights listed in Table 3.1: It ranges from 0 to only 48 kilometers at most, never exceeding 1% of the flight distance. This scenario constitutes a golden opportunity to assess empirically, the suitability and accuracy of (average) flight time as a proxy for distance between cities. Since the underlying distances for these airport pairs are essentially identical for the flat-Earth and spherical-Earth models, the validity of the empirical relationship obtained should be equally acceptable to both parties.

3.3 Flight Times Along A North-South Axis

We collect flight times over the routes in Table 3.1 from flightaware.com. These are defined as the average take-off-to-landing time over all the flights that took place over a

three-month window.[6] The data were manually collected from the website on 12 November 2022 and go as far back as 12 August 2022. We carried out an independent check over the ten most recent flights with a competitor site, airportia.com, and found negligible discrepancies of only a few minutes at most. Gate-to-gate times are slightly longer because of taxiing around the runway; flightaware.com reports those too, and they match on average what the airline itself has announced, which is yet another independent check.

Given the economic incentives for airlines, the needs of passengers and their ability to transmit and propagate information about flight arrival and departures via social networks, as well as oversight by regulatory authorities, it is simply not possible to cheat on such data systematically, let alone by a wide margin.

Airline	Route	Flight #	Flight Time	Average
Turkish Airlines	Johannesburg → Istanbul Istanbul → Johannesburg	TK41 TK40	08h42min 08h46min	08h44min
LATAM Airlines	Santiago → New York New York → Santiago	LA532 LA533	09h50min 09h33min	09h41min
Lufthansa	Frankfurt → Abuja Abuja → Frankfurt	LH594 LH595	05h37min 05h40min	05h39min
Etihad Airways	Abu Dhabi → Mahé Mahé → Abu Dhabi	EY622 EY621	04h17min 04h10min	04h13min
British Airways	London → Accra Accra → London	BA81 BA78	06h06min 06h18min	06h12min
Japan Airlines	Melbourne → Tokyo Tokyo → Melbourne	JL774 JL773	09h21min 09h33min	09h27min
Cathay Pacific	Hong Kong → Perth Perth → Hong Kong	CX171 CX170	07h01min 07h07min	07h04min
Lufthansa	Cape Town → Frankfurt Frankfurt → Cape Town	LH577 LH576	11h18min 11h07min	11h13min
Emirates Airlines	Dubai → Los Angeles Los Angeles → Dubai	EK215 EK216	15h33min 15h13min	15h23min
Qatar Airways	Doha → San Francisco San Francisco → Doha	QR737 QR738	15h02min 14h42min	14h52min

Table 3.2: Average flight times between ten airport pairs with essentially identical flat-Earth and spherical-Earth distances.

[6] The number of flight times over which we average depends on the sample size for any given route in Table 3.2; the mean and median of the twenty sample sizes are, roughly, equal to 65.

Remark 3.1 (Average Flight Time)**.** Each "flight time" in column four of Table 3.2, and later in Table 4.2, is actually an average of many individual flight times collected; but, in order to keep terminology compact, what we mean by "average flight time" listed in column five of the two tables is the average of the two "flight times" in column four (to and fro). Clearly, we need to work with this overall average flight time in order to eliminate small effects of head and tail winds. (The average to and fro times are not substantially different but can be up to 20 minutes apart.) ■

3.4 Estimating Average Flight Times by Linear Regression

Having gathered airport-pair distance data (Table 3.1) and flight time data along the same routes (Table 3.2), we are now ready to fit a model that estimates average flight time based on distance for a generic flight. Given the visible and obvious agreement between the spherical-distance column and the flat-distance column in Table 3.1, this linear regression model should be equally agreeable to flat-Earthers and spherical-Earthers alike. The model specification is grounded in the fundamental premise that engineering and economic constraints governing the modern airline industry dictate that average flight times depend on distance and little else.

(As widely reported in the popular and business press, average flight times have, counterintuitively, increased despite advances in technology; for example, see Ledsom (2022). These increases are attributed to practices like "schedule padding" and the desire to save money on fuel; recall however that our data collection window was a mere three months, obviating any issues in our case.)

The precise specification is that we stack the vector of ten North-South axis spherical-Earth distances atop the vector of ten North-South axis flat-Earth distances to construct an independent variable of dimension 20×1 that we call X. We then stack two copies of the corresponding average flight times on top of each other to construct a dependent variable of dimension 20×1 that we call Y. Finally, we regress Y (unit: hours) on a constant and X (unit: kilometers). The result is:

$$\hat{Y} = \frac{34}{60} + \frac{X}{905 \text{ km/h}} \, . \tag{3.3}$$

This means that in order to estimate average flight times, we just need to charge a constant penalty of 34 minutes for the initial climb after takeoff and the final descent before landing, and assume an average cruising speed of 905 km/h that carries the passengers from departure point to arrival point.

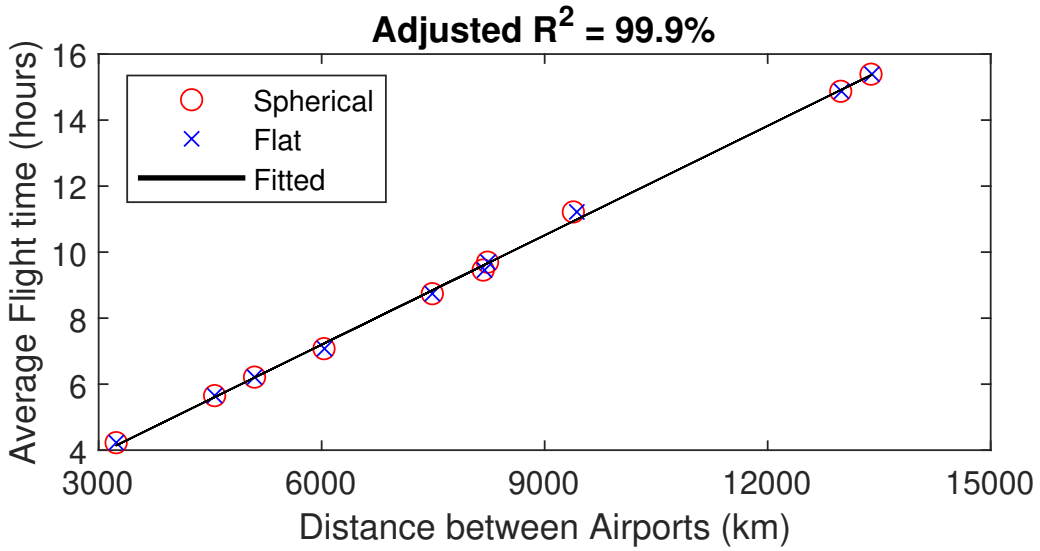

Figure 3.1: Linear regression of average flight time on a constant and distance along the North-South axis.

The adjusted R^2 of the estimated linear regression model (3.3) is a near-perfect 99.9%, so treating the relationship as exact (over the range of observed distances in the data, or slightly outside of it) seems justified.

4 Testing the Flat-Earth Model

Whereas all the work so far has been to establish commonalities between flat-Earth and spherical-Earth models, in order to calibrate an (essentially) exact relationship between flight time and distance, we now turn to the *maximal disagreement* in order to set up a powerful test, using flight times as a mutually acceptable proxy.

4.1 Geometric Analysis of Disagreement

The main difference between the two models is quite obvious: It lies in the implied circumferences of the eleven circles listed in Table 2.1. Figure 4.1 illustrates this comparison.

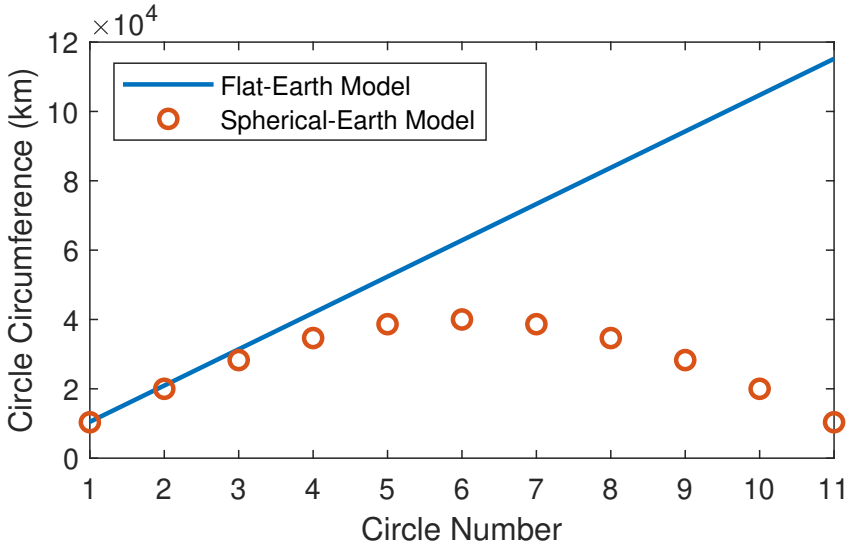

Figure 4.1: Implied circumferences of the eleven circles listed in Table 2.1 according to both models.

The two formulas used to generate Figure 4.1 are, for $k = 1, \ldots, 11$,

$$C_{\text{Flat}}(k) = 2\pi \frac{15k}{90} \times 10,000 \text{ km} \quad \text{and} \quad C_{\text{Spher}}(k) = 4\cos(90° - k \cdot 15°) \times 10,000 \text{ km} . \quad (4.1)$$

Remark 4.1 (Deviations from Perfect Sphericity)**.** The formula for $C_{\text{Spher}}(k)$ in (4.1) assumes that the Earth is a perfect sphere, in which case the circumference of the equator is four times the distance from the North Pole to the equator. The mainstream view is more nuanced: the Earth is spherical only *approximately*. It is slightly flatter around the poles, and bulges a little more around the equator. In this paper, we opt to ignore such refinements and instead treat the Earth as a perfect sphere for the sake of simplicity. ■

Initially, when one is close to the North Pole, in particular at 75° degrees of latitude, there is very little difference between the circumferences implied by both models. However, the difference gradually increases as one gets further away from the North Pole, and from Circle 6 onwards (beyond the equator into the Southern hemisphere) it is huge. This presents a golden opportunity to construct a powerful test of the flat-Earth model.

4.2 Airport Pairs on East-West Axis Far from the North Pole

Using the three criteria highlighted below:

1. departure and arrival cities linked by a direct regularly-scheduled commercial flight,
2. being as far away from the North Pole as possible,
3. and spanning an arc of longitude as wide as possible,

we put together a list of ten airline routes where the flat-Earth model should strongly disagree with the spherical-Earth model. These are presented in Table 4.1.

City	Airport	Latitude	Longitude	r (km)	θ (rad)
Santiago (Chile)	SCL	33°23′34″S	70°47′08″W	13,710	−1.24
Auckland (NZ)	AKL	37°00′29″S	174°47′30″E	14,112	3.05
Johannesburg (S. Africa)	JNB	26°08′00″S	28°15′00″W	12,904	0.49
Sydney (Australia)	SYD	33°56′46″S	151°10′38″E	13,772	2.64
São Paulo (Brazil)	GRU	23°26′08″S	46°28′23″W	12,604	−0.81
Luanda (Angola)	LAD	08°51′30″S	13°13′52″E	10,984	0.23
Papeete (France)	PPT	17°33′24″S	149°36′41″W	11,951	−2.61
Nouméa (France)	NOU	22°00′59″S	166°12′58″E	12,446	2.90
Auckland (NZ)	AKL	37°00′29″S	174°47′30″E	14,112	3.05
Perth (Australia)	PER	31°56′25″S	115°58′01E	13,549	2.02
Johannesburg (S. Africa)	JNB	26°08′00″S	28°15′00″W	12,904	0.49
Perth (Australia)	PER	31°56′25″S	115°58′01″E	13,549	2.02
Perth (Australia)	PER	31°56′25″S	115°58′01″E	13,549	2.02
Port Louis (Mauritius)	MRU	20°25′48″S	57°40′59″E	12,270	1.01
Easter Island (Chile)	IPC	27°09′53″S	109°25′18″E	13,018	−1.91
Santiago (Chile)	SCL	33°23′34″S	70°47′08″W	13,710	−1.24
Wellington (NZ)	WLG	41°19′38″S	174°48′19″E	14,592	3.05
Melbourne (Australia)	MEL	37°40′24″S	144°50′36″E	14,186	2.53
Singapore (Singapore)	SIN	01°21′33″N	103°59′22″E	9,849	1.81
Johannesburg (S. Africa)	JNB	26°08′00″S	28°15′00″W	12,904	0.49

Table 4.1: Ten airport pairs where flat-Earth and spherical-Earth models should disagree.

There is a wide variety of airports (14 in total), spanning Africa, South America, Oceania, and Asia. The average distance from the North Pole is 13,034 km, ranging from a minimum of 9,849 km (Singapore) to a maximum of 14,592 km (Wellington). Longitudes (expressed in radians) are quite different between departure and arrival airports, meaning that the routes have a strong alignment with the East-West axis instead of North-South.

4.3 Flight Times Along An East-West Axis

As in Section 3.3, we collect the average takeoff-to-landing flight times between 12 August and 12 November 2022 from flightaware.com. These are reported in Table 4.2.[7]

Airline	Route	Flight #	Flight Time	Average
LATAM Airlines	Santiago → Auckland	LA801	12h04min	11h08min
	Auckland → Santiago	LA800	10h11min	
Qantas Airways	Johannesburg → Sydney	QF64	11h16min	12h28min
	Sydney → Johannesburg	QF63	13h40min	
Angola Airlines	São Paulo → Luanda	DT748	7h58min	8h08min
	Luanda → São Paulo	DT747	8h17min	
Aircalin	Papeete → Nouméa	SB601	6h06min	5h36min
	Nouméa → Papeete	SB600	5h06min	
Air New Zealand	Auckland → Perth	NZ175	6h41min	6h11min
	Perth → Auckland	NZ176	5h40min	
Qantas Airways	Johannesburg → Perth	QF66	8h57min	9h49min
	Perth → Johannesburg	QF65	10h40min	
Air Mauritius	Perth → Port Louis	MK441	7h50min	7h03min
	Port Louis → Perth	MK440	6h17min	
LATAM Airlines	Easter Island → Santiago	LA842	4h13min	4h29min
	Santiago → Easter Island	LA841	4h44min	
Qantas Airways	Wellington → Melbourne	QF172	3h34min	3h21min
	Melbourne → Wellington	QF171	3h09min	
Singapore Airlines	Singapore → Johannesburg	SQ478	9h58min	9h58min
	Johannesburg → Singapore	SQ479	9h59min	

Table 4.2: Flight times for ten airport pairs where flat-Earth and spherical-Earth models should disagree.

The majority of these routes depart from and/or arrive in Australia or New Zealand.

4.4 Statistical Analysis

We have now gathered all the building blocks to construct an estimator of Earth's curvature, along with corresponding inference. In order to conduct the analysis, we map distances

[7]The number of flight times over which we average depends on the sample size for any given route in Table 4.2; both the mean and median of the twenty sample sizes are, roughly, equal to 50.

into flight times using the calibration of Section 3.4:

$$T\big(r_{i,1},\theta_{i,1};r_{i,2},\theta_{i,2};c\big) \coloneqq \frac{34}{60} + \frac{D\big(r_{i,1},\theta_{i,1};r_{i,2},\theta_{i,2};c\big)}{905 \text{ km/h}} \ , \tag{4.2}$$

where $(r_{i,1},\theta_{i,1})$ are the polar coordinates of the first-listed airport on route $i = 1,\ldots,10$ (see the last two columns of Table 4.1), $(r_{i,2},\theta_{i,2})$ are the polar coordinates of the second-listed one, D is the integrated formula for distance from Theorem 2.3, and c is the (*a priori* unknown) curvature. The curvature c is then estimated via nonlinear least squares:

$$\hat{c} \coloneqq \operatorname*{argmin}_c \sum_{i=1}^{10} \big[Y_i - T(r_{i,1},\theta_{i,1};r_{i,2},\theta_{i,2};c)\big]^2$$

where Y_i is the average flight time for route i, as recorded in the last column of Table 4.2, and c can range over the domain $\big[0, \min(\min_i(\pi/r_{i,1}), \min_i(\pi/r_{i,2}))\big]$. The results are as follows:

$$\hat{c} = 1.578 \cdot 10^{-4} \quad \text{and} \quad \mathrm{SE}(\hat{c}) = 4.981 \cdot 10^{-7} \ ,$$

where the standard error $\mathrm{SE}(\hat{c})$ is computed according to Greene (2008, Theorem 11,2); note that we use the degree-of-freedom correction for $\hat{\sigma}^2$ (with $K = 1$) outlined below Greene (2008, Equation (11-13)).

An asymptotic (or standard-theory) nominal 95% confidence interval for c is then obtained as

$$\hat{c} \pm t_{9,0.975} \cdot \mathrm{SE}(\hat{c}) = [1.567 \cdot 10^{-4}, 1.589 \cdot 10^{-4}] \ , \tag{4.3}$$

where $t_{n,\lambda}$ denotes the λ quantile of the t-distribution with n degrees of freedom. (Some might use $z_{0.975} = 1.96$, the 0.975 quantile of the standard normal distribution, instead of $t_{9,0.975} = 2.262$ in the construction of the asymptotic confidence interval (4.3) but we prefer to 'err' on the conservative side by using a wider interval.)

Alternatively, one can use the studentized symmetric bootstrap based on resampling cases; for example, see Davison and Hinkley (1997, Sections 6.2 and 7.4). In this way one obtains a nominal 95% confidence interval as

$$\hat{c} \pm t^{|\cdot|,*}_{0.95} \cdot \mathrm{SE}(\hat{c}) = [1.565 \cdot 10^{-4}, 1.591 \cdot 10^{-4}] \ . \tag{4.4}$$

Here $t^{|\cdot|,*}_{\lambda}$ denotes the bootstrap estimate of the λ quantile of the sampling distribution of

$$\frac{|\hat{c} - c|}{\mathrm{SE}(\hat{c})} \ .$$

As is often the case with small sample sizes, the bootstrap confidence interval is somewhat wider than the asymptotic confidence interval, the reason being that

$$t^{|\cdot|,*}_{0.95} = 2.580 > 2.262 = t_{9,0.975} = t^{|\cdot|}_{9,0.95} \ ,$$

where $t_{n,\lambda}^{|\cdot|}$ denotes the λ quantile of $|X|$ with $X \sim t_n$.

Nevertheless, both intervals came to the same conclusion: Whereas the flat-Earth model is rejected, the spherical-Earth model is not. This is because both intervals do not contain zero but do contain $c^* := \pi/20,000 = 1.571 \cdot 10^{-4}$.

Another way to carry out inference on the flat-Earth model is to compute a p-value for the hypothesis testing problem

$$H_0 : c = 0 \quad \text{vs.} \quad H_0 : c > 0 \ .$$

Both asymptotic theory and the bootstrap yield a p-value < 0.001, so that the flat-Earth model is resolutely rejected by the data.

Last but not least, by inverting the endpoints of the confidence intervals (4.3)–(4.4) for Earth's curvature c one can back out nominal 95% asymptotic and bootstrap confidence intervals for Earth's radius $1/c$ as

$$[6,293 \text{ km}, 6,383 \text{ km}] \quad \text{respectively} \quad [6,286 \text{ km}, 6,390 \text{ km}] \ . \tag{4.5}$$

Since the point estimate of Earth's radius is given by $1/\hat{c} = 1/1.578 \cdot 10^{-4} = 6{,}338$ km, even the somewhat wider bootstrap confidence interval implies a relative accuracy of 99.2%, where we define *relative accuracy* as one minus the ratio of margin of error to point estimate. For a symmetric confidence interval, the margin of error is given by half the width of the interval, that is, by the distance from the point estimate to either end point of the interval. The two confidence intervals in (4.5) for $1/c$ are not symmetric anymore due to the nonlinear operation of inverting the endpoints of the symmetric intervals for c. To be conservative, we thus take the larger of the two distances from the point estimate to either end point, which results in the following relative accuracy based on the bootstrap confidence interval: $1 - (6,390 - 6,338)/6,338 = 0.9918$.

4.5 Discussion

The results of our statistical analysis have been obtained by making some simplifying assumptions:

1. In the spherical-Earth model, the Earth is perfectly spherical.
2. The meter is exactly $\frac{1}{10{,}000{,}000^{\text{th}}}$ of the distance from the North Pole to the equator.
3. The mapping from distances to average flight times estimated via linear regression on North-South routes was used as if it held perfectly.
4. The small sample ($n = 10$) that we have collected synthesizes the information content of the other regularly-scheduled commercial airline routes not downloaded.

Having said that, none of these limitations, even taken together, really matter in the end: Even if we increased the widths of the confidence intervals (4.3)–(4.4) by a factor of ten, the flat-Earth model would still be rejected.

Our contribution to a topic uniquely intriguing in both scientific discourse and in popular culture, is that we managed to conclusively discriminate between two strongly opposing physics models without doing any physics experiment or physics theory. Rather, we simply and carefully applied the statistical method. It is usually hard to change one's mind (let alone someone else's mind) about a belief held; but for the proponents of the flat-Earth model, we suggest an easy way to do so: Take one of the flights listed in Table 4.2 and time it with your own watch. (Strictly speaking, take a round-trip flight and then record the average of the two flight times.)

Sometimes a simple picture that distills the essence of the result is a good way to summarize the main point. There are two flights from Perth (Western Australia) that take almost exactly seven hours on average: due North to Hong Kong, and due West to Mauritius. Given near-identical average flight durations, the distances should match too. They do not if the Earth is flat, but they do if it is spherical, as Figure 4.2 illustrates.

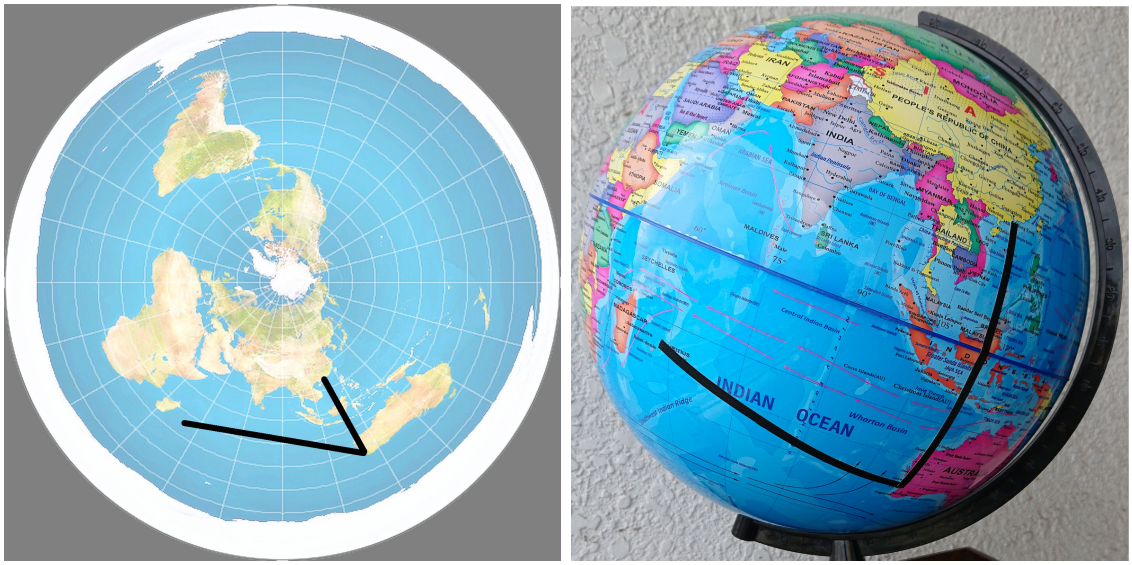

Figure 4.2: Perth–Hong Kong and Perth–Mauritius lines drawn in black on both maps.

If the Earth were flat, Perth–Mauritius should take twice as long as Perth–Hong Kong, which it does not. The fundamental contradiction is that, under the flat-Earth model, flight durations observed on an East-West axis far away from the North Pole are incompatible with flight durations observed on a North-South axis.

5 Conclusion

We have carried out a side-by-side evaluation of the unorthodox flat-Earth model against the orthodox spherical-Earth model, without *a priori* favoring one over the other. The key was to use, as an instrument, the distance between pairs of airports connected by regularly-scheduled commercial flights, whose times of departure and arrival are essentially unfalsifiable public knowledge.

We first selected airport pairs of locations for which both models give the same distance, namely airport pairs on the North-South axis that are either on the same meridian or on an antemeridian with a combined distance from the North Pole less than or equal to 20,000 km. We used these selected routes along the North-South axis (allowing for North Pole flyover) to calibrate a simple linear regression connecting distance to flight duration in a way that should be equally acceptable to the proponents of both the flat-Earth model and the spherical-Earth model. We then selected flight routes along the East-West axis far away from the North Pole to set up a powerfully discriminant test between the two models.

The outcome is that observed flight durations along the East-West axis are too short to be compatible with those along the North-South axis if the Earth is flat. This test decisively rejects the flat-Earth model in favor of the spherical-Earth model. Our unique test's main and compelling advantages are (i) its simple yet powerful design; (ii) its use of easily verifiable and uncontroversial data; and (iii) the fact that it was executed in an even-handed and disinterested way.

Last but not least, we have demonstrated that the statistical methods can estimate a physics quantity as important as Earth's curvature with a remarkably high relative accuracy of 99.2% without using *any* physics whatsoever.

References

Davison, A. C. and Hinkley, D. V. (1997). *Bootstrap Methods and Their Application*. Cambridge University Press, Cambridge.

Edney, M. H. and Pedley, M. S. (2020). Writing cartography's enlightenment. *The Cartographic Journal*, 57(4):312–334.

Greene, W. H. (2008). *Econometric Analysis*. Pearson, Upper Saddle River, New Jersey, sixth edition.

Kells, L. M., Kern, W. F., and Bland, J. R. (1940). *Plane and Spherical Trigonometry*. McGraw-Hill, New York and London, second edition.

Kuzii, O. and Rovenchak, A. (2019). What the gravitation of a flat Earth would look like and why thus the Earth is not actually flat. *European Journal of Physics*, 40(3):035008.

Ledsom, A. (2022). Why is your flight slower today than ever before? *Forbes*. https://www.forbes.com/sites/alexledsom/ (published on 08-December-2022).

Rowbotham, S. B. (1881). *Zetetic Astronomy: Earth Not a Globe*. London, third edition.

Snyder, J. P. (1987). *Map Projections – A Working Manual*. U.S. Geological Survey #1395.

A Mathematical Proofs

A.1 Proof of Proposition 2.1

Regarding the first two statements, the expression between square brackets is called the *colatitude* of the point, expressed in decimal degrees. Rescaling by $\pi/180°$ converts it into radians. If the Earth is spherical with distance from the North Pole to the equator $10,000$km, then Equations (2.2–2.3) follow. If the Earth is flat, due to the fact that the polar azimuthal equidistant projection preserves distances along meridians, the equations also hold.

Regarding the last two statements, they are just conversion from the degrees/minutes/seconds formalism to decimal degrees to radians. The sign comes from the trigonometric convention that turning counterclockwise is positive.

A.2 Proof of Theorem 2.1

The first step of the proof is to convert the polar coordinates (r_i, θ_i) into Cartesian coordinates centered on the North Pole. In this layout, from Figure 2.1 we see that the Greenwich Meridian (0°) lies on the vertical axis in the direction of negative ordinates, and the antimeridian (180°) on the same axis in the direction of positive ordinates. The horizontal axis encompasses the 90° East meridian in the direction of positive abscissae, and the 90° West meridian in the direction of negative abscissae. From this we deduce that the Cartesian coordinates of points P_1 and P_2 are as follows:

$$x_1 = r_1 \sin(\theta_1) \qquad y_1 = -r_1 \cos(\theta_1) \tag{A.1}$$

$$x_2 = r_2 \sin(\theta_2) \qquad y_2 = -r_2 \cos(\theta_2) \tag{A.2}$$

From Equations (A.1–A.2), we deduce the Euclidean distance between points P_1 and P_2:

$$\begin{aligned} d^{\mathrm{F}}(r_1, \theta_1; r_2, \theta_2) &= \sqrt{(x_2 - x_1)^2 + (y_2 - y_1)^2} \\ &= \sqrt{[r_2 \sin(\theta_2) - r_1 \sin(\theta_1)]^2 + [r_2 \cos(\theta_2) - r_1 \cos(\theta_1)]^2} \\ &= \sqrt{r_1^2 + r_2^2 - 2r_1 r_2 [\sin(\theta_1)\sin(\theta_2) + \cos(\theta_1)\cos(\theta_2)]} \\ &= \sqrt{r_1^2 + r_2^2 - 2r_1 r_2 \cos(\theta_1 - \theta_2)}\ , \end{aligned} \tag{A.3}$$

where the last line uses the classic trigonometric identity for angle subtraction.

A.3 Proof of Theorem 2.2

The shortest path between two points on the spherical Earth is the shorter arc of a great circle that joins these two points. Great circles lie on the surface of the Earth and have the same center as the Earth. To join two points $P_1 := (r_1, \theta_1)$ and $P_2 := (r_2, \theta_2)$, there exists a unique great circle, except in the special cases where P_1 and P_2 are identical or antipodal. All great circles have circumference $40,000$km (four times the distance from the North Pole to the equator) and radius $\rho = 20,000\text{km}/\pi$. Thus, to obtain the distance between P_1 and P_2, it is sufficient to determine the angular length a of the arc between these two points along the great circle that joins them. This is achieved by the *law of cosines* (see, e.g., Kells et al. (1940), §156, Equation (18), p. 315):

$$\cos a = \cos(\lambda_1)\cos(\lambda_2) + \sin(\lambda_1)\sin(\lambda_2)\cos(\theta_1 - \theta_2) \ . \tag{A.4}$$

On this basis, we see that $d^{\text{S}}(r_1, \theta_1; r_2, \theta_2)$ is equal to

$$\frac{20,000\text{km}}{\pi} \arccos\big[\cos(\lambda_1)\cos(\lambda_2) + \sin(\lambda_1)\sin(\lambda_2)\cos(\theta_1 - \theta_2)\big] \ . \tag{A.5}$$

Thanks to the classic trigonometric identities

$$\sin x \sin y = \frac{\cos(x-y) - \cos(x+y)}{2}, \quad \cos x \cos y \ = \frac{\cos(x - yb) + \cos(x+y)}{2}, \tag{A.6}$$

we conveniently rearrange the spherical-Earth distance $d^{\text{S}}(r_1, \theta_1; r_2, \theta_2)$ as

$$\frac{1}{c^*} \arccos\left[\frac{1+\cos(\theta_2 - \theta_1)}{2}\cos(\lambda_1 - \lambda_2) + \frac{1-\cos(\theta_2-\theta_1)}{2}\cos(\lambda_1+\lambda_2)\right] \ . \tag{A.7}$$

Using other some other classic trigonometric identities,

$$\frac{1+\cos x}{2} = \cos^2\left(\frac{x}{2}\right), \quad \frac{1-\cos x}{2} = \sin^2\left(\frac{x}{2}\right) \ , \tag{A.8}$$

we end up with $d^{\text{S}}(r_1, \theta_1; r_2, \theta_2)$ being equal to

$$\frac{1}{c^*}\arccos\left[\cos^2\left(\frac{\theta_1-\theta_2}{2}\right)\cos\big(\lambda_1 - \lambda_2\big) + \sin^2\left(\frac{\theta_1-\theta_2}{2}\right)\cos\big(\lambda_1+\lambda_2\big)\right] \tag{A.9}$$

$$= \frac{1}{c^*}\arccos\left[\cos^2\left(\frac{\theta_1-\theta_2}{2}\right)\cos\big(\lambda_1 - \lambda_2\big) + \sin^2\left(\frac{\theta_1-\theta_2}{2}\right)\cos\big(\lambda_1+\lambda_2\big)\right] \tag{A.10}$$

$$= \frac{1}{c^*}\arccos\left\{\cos^2\left(\frac{\theta_1-\theta_2}{2}\right)\cos\big[(r_1 - r_2)c^*\big] + \sin^2\left(\frac{\theta_1-\theta_2}{2}\right)\cos\big[(r_1+r_2)c^*\big]\right\} \ ,$$

and thus the proof of Theorem 2.2 is complete.

A.4 Proof of Theorem 2.3

What needs to be proven is that

$$\lim_{c \searrow 0} D(r_1, \theta_1; r_2, \theta_2; c) = \sqrt{r_1^2 + r_2^2 - 2r_1 r_2 \cos(\theta_1 - \theta_2)} \; . \tag{A.11}$$

From the Taylor series expansion of the cosine around zero:

$$\cos(\varepsilon) = 1 - \frac{\varepsilon^2}{2} + o\big(\varepsilon^2\big) \quad \text{and} \quad \arccos\left(1 - \frac{\varepsilon^2}{2}\right) = \varepsilon + o\big(\varepsilon\big) \; . \tag{A.12}$$

Remembering also that $\sin(\varepsilon) = \varepsilon + o(\varepsilon)$, we start from a variant of Equation (A.5):

$$\begin{aligned} &\cos(r_1 c)\cos(r_2 c) + \sin(r_1 c)\sin(r_2 c)\cos(\theta_1 - \theta_2) \\ &\quad = \left(1 - \frac{r_1^2 c^2}{2}\right)\left(1 - \frac{r_2^2 c^2}{2}\right) + \big(r_1 c\big)\big(r_2 c\big)\cos(\theta_1 - \theta_2) + o\left(c^2\right) &\text{(A.13)} \\ &\quad = 1 - \frac{r_1^2 + r_2^2 - 2r_1 r_2 \cos(\theta_1 - \theta_2)}{2}\, c^2 + o\left(c^2\right) &\text{(A.14)} \\ &\arccos\big[\cos(r_1 c)\cos(r_2 c) + \sin(r_1 c)\sin(r_2 c)\cos(\theta_1 - \theta_2)\big] \\ &\quad = \sqrt{r_1^2 + r_2^2 - 2r_1 r_2 \cos(\theta_1 - \theta_2)}\; c + o(c) \; , &\text{(A.15)} \end{aligned}$$

from which we deduce $\lim_{c \searrow 0} D(r_1, \theta_1; r_2, \theta_2; c) = \sqrt{r_1^2 + r_2^2 - 2r_1 r_2 \cos(\theta_1 - \theta_2)}$.

A.5 Proof of Theorem 3.1

Let us remind the reader that the arc-cosine is a strictly decreasing function that maps $[-1, 1]$ into $[0, \pi]$. Thus, $\arccos\big[\cos(x)\big] = x$ if and only if $x \in [0, \pi]$. We start with the same-meridian case $\theta_1 = \theta_2$ (modulo 2π).

$$\begin{aligned} d^{\mathrm{F}}\big(r_1, \theta_1; r_2, \theta_2\big) &= \sqrt{r_1^2 + r_2^2 - 2r_1 r_2} = |r_1 - r_2| &\text{(A.16)} \\ d^{\mathrm{S}}\big(r_1, \theta_1; r_2, \theta_2\big) &= \frac{1}{c^*} \arccos\big\{\cos\big[(r_1 - r_2)c^*\big]\big\} &\text{(A.17)} \\ &= \frac{1}{c^*} \arccos\big\{\cos\big[|r_1 - r_2|c^*\big]\big\} = |r_1 - r_2| &\text{(A.18)} \end{aligned}$$

Next, we turn to the antimeridian case $\theta_1 = \theta_2 + \pi$ (modulo 2π).

$$\begin{aligned} d^{\mathrm{F}}\big(r_1, \theta_1; r_2, \theta_2\big) &= \sqrt{r_1^2 + r_2^2 + 2r_1 r_2} = r_1 + r_2 &\text{(A.19)} \\ d^{\mathrm{S}}\big(r_1, \theta_1; r_2, \theta_2\big) &= \frac{1}{c^*} \arccos\big\{\cos\big[(r_1 + r_2)c^*\big]\big\} &\text{(A.20)} \end{aligned}$$

This case splits into two sub-cases. The first sub-case is defined by $r_1 + r_2 \leq 20,000\text{km}$, implying that $(r_1 + r_2)c^* \leq \pi$, so we have:

$$d^{\mathrm{S}}\big(r_1, \theta_1; r_2, \theta_2\big) = \frac{1}{c^*} \arccos\big\{\cos\big[(r_1 + r_2)c^*\big]\big\} = r_1 + r_2 \; . \tag{A.21}$$

This corresponds to flying over the North Pole, which is possible in the spherical-Earth model and also in the flat-Earth model. The second sub-case is defined by $r_1 + r_2 > 20,000\text{km}$, implying that $(r_1 + r_2)c^* > \pi$, so we have:

$$d^{\text{S}}\big(r_1, \theta_1; r_2, \theta_2\big) = \frac{1}{c^*} \arccos\big\{\cos\big[(r_1 + r_2)c^*\big]\big\} \tag{A.22}$$

$$= \frac{1}{c^*} \arccos\big\{2\pi - \cos\big[(r_1 + r_2)c^*\big]\big\} = 40,000\text{km} - (r_1 + r_2)\ . \tag{A.23}$$

This corresponds to flying over the South Pole, which is impossible if the Earth is flat.

B More Representations of the Flat-Earth Map

The geometry of Figure 2.1 goes back at least to Cassini's 1696 publication of the map shown in Figure B.1. It depicts what was drawn on the floor of the Paris Observatory at the time. The Paris Observatory is also noteworthy in that, a century later, it hosted the first platinum meter bar that was to become the universal reference for the unit of distance, defined as the $\frac{1}{10{,}000{,}000^{\text{th}}}$ part of the distance from the North Pole to the equator.

Figure B.1: Map of the continents and oceans according to Cassini.

Technically speaking, this is known as the *polar azimuthal equidistant projection*. It means that distances from the North Pole to any point on Earth are preserved, and longitudes are also preserved. In France, it is known as the "Postel" projection, after the local 16th-century astronomer who pioneered it; see Edney and Pedley (2020, pp. 326–328) for comprehensive historical background.

Closer to our times, the emblem of the United Nations, which also features on its flag, adopts the same flat-Earth projection, as shown in Figure B.2.

Figure B.2: Emblem of the United Nations.

This is not to say that the renowned French astronomers Cassini and Postel, and all the founding members of the United Nations believed that the Earth is flat. Our point is that there are strong reasons for proponents of the flat-Earth model to adopt the polar azimuthal equidistant projection as their map.

The map in Figure 2.1 was collected from the official site of the Flat Earth Society at

http://theflatearthsociety.org/home/index.php/about-the-society/faq

This webpage has been archived dozens of times on http://archive.org, the "Wayback Machine", including recently on 22 September 2022 at 19:55:58. The origins of the modern flat-Earth movement can be traced back to Rowbotham (1881, Figure 54), so we also reproduce his map below.

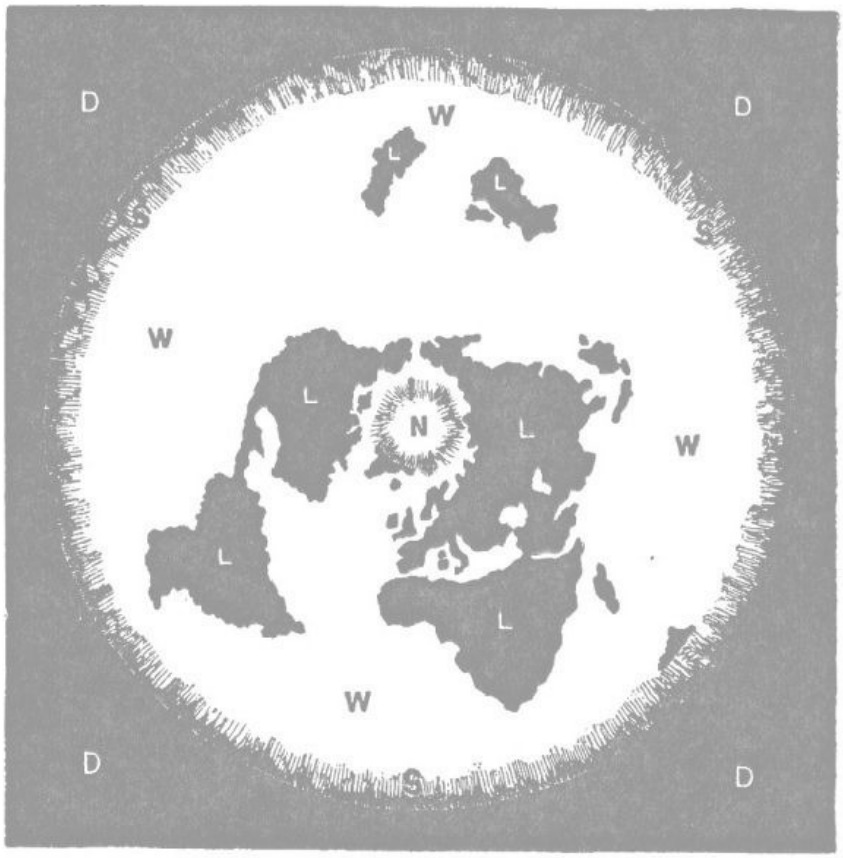

Figure B.3: Classic XIXth-century map from a leading proponent of the flat-Earth model.

C Homemade Sanity Check for Map Scale

We now address a potential objection, which is that Figure 2.1 lacks a kilometric scale. In and of itself, this is a bit of a handicap for the flat-Earth model because it means that it is not a fully specified model — whereas the spherical-Earth model is. This handicap is not insurmountable, as we were able to complete the flat-Earth model by using the very definition of the meter in Equation (2.1). Still, some people may remain unconvinced and, for example, claim that 'the Earth is much smaller than we think' or 'the Earth is much bigger than we think'. In this case, the kilometric distances from the North Pole listed in the fourth column of Table 2.1 could be, say, 50% smaller, or twice as large (although they would all have to be rescaled by the same coefficient of proportionality).

This potential objection is easily addressed by noticing that both models also agree about distances between any two cities on the same meridian, due to the nature of the polar azimuthal equidistant projection. Therefore, it is sufficient to purchase a privately-produced roadmap, measure the distance between two towns on the same meridian, and

compare it to the theoretical number implied by Equations (2.1). France, in particular, has a long history in the development of the automobile, including Grand Prix racing (now called Formula One), and the production of high-performance tires through the old multinational company Michelin. In order to promote the use of cars (and of tires), the Michelin family has since the beginning sponsored the production of the world-famous Michelin guide for restaurants, awarding Michelin stars very gingerly, and also a full complement of Michelin road maps. They can hardly be suspected of fraud, as (before the recent development of onboard GPS devices) French drivers mostly relied on Michelin's kilometric measurements to complete their trips, and every car has an odometer against which accuracy can be checked.[8]

The meridian at longitude 2° East traverses France nearly from its Northermost tip on the English Channel to its Southernmost tip on the Spanish border. We can pick two small communes on this meridian: Créquy (Pas-de-Calais, postal code 62310), which is located at 50°30′ North, and Sonnac-sur-l'Hers (Aude, postal code 11230), which is located at 43° North. Thus, the difference in latitudes, 7°30′, is exactly $1/12^{\text{th}}$ of the distance between the North Pole and the equator (Circle 6). According to the official definition of the meter embedded inside Equation (2.1), it should be $\frac{10{,}000}{12} = 833$ kilometers.

To run a crude sanity check with readily-available materials, we applied a hand-held ruler onto the 2017 Michelin map of France, reference code '721 National'. We personally measured the distance between these two towns. It turned out to be 83 centimeters, as shown in Figure C.1 below.

At the 1:1,000,000 scale specified on the map (1 cm = 10 km), this corresponds to roughly 830 km. Thus, a crude — but robust — sanity check confirms Table 2.1 independently: The Earth cannot be 'much smaller than we think' or 'much bigger than we think' because otherwise the Michelin maps of France would have been unusable for motorists during all these years.

Note that France is ideal for running such a 'hands-on' experiment because the country is so small ($1,000 \times 1,000$ km) that its maps under the flat-Earth model and the spherical-Earth model would look almost indistinguishable from one another: Curvature would have negligible impact, especially around the 45° North parallel (a.k.a. Circle 3 in the nomenclature of Table 2.1).

[8]The second author has done so himself since being old enough to get a driver's license.

Figure C.1: Manual confirmation that the meter is the $\frac{1}{10{,}000{,}000^{\text{th}}}$ part of the distance between the North Pole and the equator. The distance between Créquy (yellow square at the Northern end) and Sonnac-sur-l'Hers (orange square at the Southern end) is approximately 83 centimeters, with a map scale of 1 cm = 10 km.